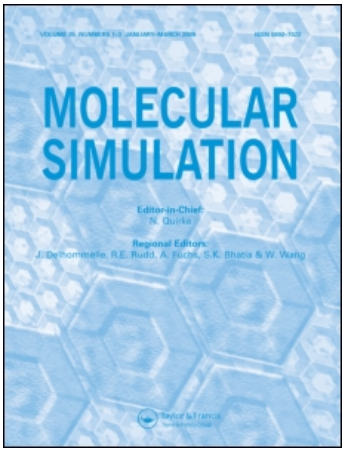

Molecular Simulation
Publication details, including instructions for authors and subscription information:
http://www.informaworld.com/smpp/title~content=t713644482

Electrostatic Attraction and/or Repulsion Between Charged Colloids: A (NVT) Monte-Carlo Study

A. Delville[a]; R. J. -M. Pellenq[a]
[a] Centre de Recherche sur la Matière Divisée, CNRS et Université d'Orléans, Orléans cedex 02, France

To cite this Article Delville, A. and Pellenq, R. J. -M.(2000) 'Electrostatic Attraction and/or Repulsion Between Charged Colloids: A (NVT) Monte-Carlo Study', Molecular Simulation, 24: 1, 1 — 24
To link to this Article: DOI: 10.1080/08927020008024184
URL: http://dx.doi.org/10.1080/08927020008024184

Molecular Simulation, 2000, Vol. 24, pp. 1–24
Reprints available directly from the publisher
Photocopying permitted by license only

ELECTROSTATIC ATTRACTION AND/OR REPULSION BETWEEN CHARGED COLLOIDS: A (NVT) MONTE-CARLO STUDY

A. DELVILLE* and R. J.-M. PELLENQ

Centre de Recherche sur la Matière Divisée, CNRS et Université d'Orléans, 45071 Orléans cedex 02, France

(Received April 1999; accepted July 1999)

We have performed canonical Monte-Carlo simulation of the distribution of counter-ions between two uniformly charged colloids of different geometries (infinite slabs, discoids and spheres). We have calculated the net force (or the pressure) between the colloids as a function of the interparticle separation in order to determine their stability. Simulations were performed within the primitive model which describes short-ranged excluded volume effects and long-ranged electrostatic interactions. Long-ranged behavior of the Coulomb potential has been handle by different numerical procedures: Ewald summations, hypersphere's method or external self-consistent field's approximation. In all cases, the net force between a pair of colloids results from the balance between the electrostatic attraction and the contact repulsion exerted by the condensed counter-ions. In the case of two infinite slabs, both contributions are (in absolute value) of the same order of magnitude; the resulting net force depends on the so-called electrostatic coupling which is the ratio of the counter-ion/surface electrostatic term at contact divided by the thermal energy. At high coupling (high surface density, polyvalent ions and/or low dielectric constant), we have demonstrated the existence of an attractive domain responsible for the cohesion of various lamellar materials (calcic-clay, cement, organic dispersion...). At low coupling (monovalent counterions in water), we have only detected a monotonous swelling behavior (repulsion) of the charged interfaces. We discuss these results on the basis of ionic correlations within the double-layers of condensed counter-ions. In addition to the infinite-slab case, we present results for a pair of discoid and spherical colloids in order to evaluate finite-size effects. By contrast to infinite interfaces, the electrostatic attraction is found to be negligible for a pair of parallel discoids neutralized by monovalent counter-ions (weak coupling conditions); the net force is then repulsive and driven by the contact force. A net attraction is also found in the case of divalent counter-ions (strong coupling conditions). No attractive regime is found in the case of interacting spheres neutralized by monovalent counter-ions.

Keywords: Charged colloids; Monte-Carlo simulation

*Corresponding author.

1. INTRODUCTION

Charged colloids constitute a large class of materials implied in numerous industrial applications (waste management, water treatment, drilling, paint, food and cosmetic industry, civil engineering, heterogeneous catalysis, ...) exploiting their various physico-chemical properties (adsorption, ionic exchange capacity, surface acidity, swelling or cohesive behavior, ...). For that reason, the stability of emulsions of charged colloids was the subject of numerous experimental [1 – 3, 19] and theoretical [4 – 17] studies. Because of the long range of the electrostatic potential, a reduced fraction of charged colloids totally modifies the mechanical behavior of dispersed materials. As a consequence, the approximate Deryaguin-Landau-Verwey-Overbeek (D.L.V.O.) theory was early introduced in order to describe the long-ranged electrostatic coupling within suspensions of charged colloids.

In that theory, the stability of suspensions of charged colloids results from a balance between short-ranged van der Waals attraction and long ranged electrostatic repulsion. This entropic repulsion is the consequence of the overlap between the diffuse layers of counterions surrounding each polyion. We thus performed numerical simulations of the net interactions between charged interfaces in the framework of the primitive model (short-ranged excluded volume and long-range electrostatic coupling). Our Monte-Carlo simulations were performed in the (N, V, T) ensemble for various conditions (electric surface charge density, ionic radius and charge, shape and size of the polyions).

From the simulations, we determined the mechanical stability of the interfaces without using any approximation in order to determine the domain of validity of the D.L.V.O. theory. The entropic repulsion included in that simple theory is responsible for the stability of charged colloids at low electrostatic coupling ($\xi = |\sigma_w q/R_{\text{hyd}}/(4\varepsilon_0\varepsilon_r kT)$, where σ_w is the surface charge density, q the ionic charge and R_{hyd} the ionic radius). But for infinite charged lamellae, electrostatic attraction [4 – 11, 13 – 17] and contact repulsion [13 – 17] were also shown to occur and drive the mechanical behavior of the colloid suspension under conditions of strong electrostatic coupling ($\xi > 0.4$) and large ionic coverage ($\eta = 16\pi|\sigma_w|R_{\text{hyd}}^2/(3L|q|)$) respectively ($L$ is the interlamellar separation). These attracto/repulsive behaviors are both due to ionic correlations and are neglected in the Poisson-Boltzmann treatment of charged interfaces, although this approximation underlies the D.L.V.O theory.

Despite of the simplicity of the primitive model, we predicted complex phase diagrams and equations of state, corresponding to the behavior of

various charged lamellar materials (clays, cement, pillared and organo clays,...). We further investigate the influence of the size and shape of the polyions on the nature of their electrostatic coupling.

2. SIMULATION METHODS

We have used the (*NVT*) Monte-Carlo simulation technique in order to investigate the equation of state (net force *versus* inter-colloid distance) of a pair of charged colloids immersed in an solvent. In our study, the solvent reduces to a dielectric continuum containing the number of counter-ions necessary to maintain the electroneutrality of the system. In this work, we have considered three different geometries for the colloids namely two infinite slabs, a pair of discoids and a pair of spherical colloids. Through out this work, the temperature is fixed at 298 K and the solvent dielectric constant is set equal to 78.5 (bulk water) or 5 (organic solvent).

2.1. Infinite Slabs

In the case of two infinite slabs, the lamellae are structureless with a uniform surface density of charge (σ_w) and the counter-ions are described as hard spheres characterized by their (hydrated) radius R_{hyd} and charge q. This corresponds to a crude but simple modelling of clays or cement materials (each material being characterized by its surface density of charge) within the frame of the primitive model.

2.1.1. Calculation of the Potential Energy

The simulations were run within the frame of the Canonical ensemble *i.e.*, at fixed number of ions, volume and temperature. The generation of the Markov chain of configurations in Monte-Carlo simulations depends on the total interaction energy which is the sum of the ion–ion and the ion-wall interactions. The simulation study of the equation of state of two infinite slabs was carried out by using two different approaches: the so-called euclidian [4, 6, 9, 10] and hyperspherical [13] methods respectively. In euclidian geometry, the simulation box volume is defined by the interlamellar distance and by the lateral extension in the directions parallel to the slabs. Periodic boundary conditions and minimum image convention were only applied in the directions parallel to the slabs (the minimum image convention introduces a cut-off in the ion–ion potential calculation at half the

simulation cell lateral size). The ion–ion potential for two kl ions separated by a distance r_{kl} is therefore written as:

$$U^{ii}(r_{kl}) = \frac{q^2}{4\pi\varepsilon_0\varepsilon_r r_{kl}} \quad \text{for } r_{kl} > a$$
$$U^{ii}(r_{kl}) = \infty \quad \text{for } r_{kl} \leq a \tag{1}$$

where d is the (solvated) ionic diameter ($d = 2R_{\text{hyd}}$). The ion-wall potential is given by:

$$U^{iw}(\Delta z) = \frac{q\sigma_w W}{4\pi\varepsilon_0\varepsilon_r} G(Z), \quad Z = \left(\frac{\Delta z}{W}\right) \tag{2}$$

$$G(Z) = 4\ln\left\{\frac{\sqrt{(1/2)+Z^2}+(1/2)}{\sqrt{(1/4)+Z^2}}\right\} - Z\left[\pi + 2\arcsin\left(-\frac{((1/4)+Z^2)^2+(1/8)}{((1/4)+Z^2)^2}\right)\right] \tag{3}$$

Δz is the ion-wall distance. Relations (1) and (2) hold for all ions in the simulation box of volume $V = W^2L$ where W is the lateral box size and L the separation between the walls (see Fig. 1). W is directly related to the total number of the counter-ions inclosed in the inter-layer space N, their electric charge q, and the surface charge density σ_w through the following equation:

$$W = \sqrt{\frac{-Nq}{2\sigma_w}} \tag{4}$$

This equation states the electroneutrality of the system: the total ionic charge compensates exactly for the charge onto the walls. Due to the relatively small size of the simulation box compared to the characteristic length of coulombic interactions, it is necessary to include some corrections in order to calculate accurately the system energy. One way to achieve this [4, 6, 10], is to consider infinite virtual charged sheets placed at regular separation parallel to and in-between the two walls (see Fig. 1). A square hole is cut in each virtual sheet in order to not count twice the various electrostatic contributions in the simulation cell. The surface charge density σ_{ext} of those sheets is obtained in a self-consistent manner from the block-averaged ionic density profile (12) in the direction perpendicular to the walls. The interaction between an ion in the simulation box and one of these

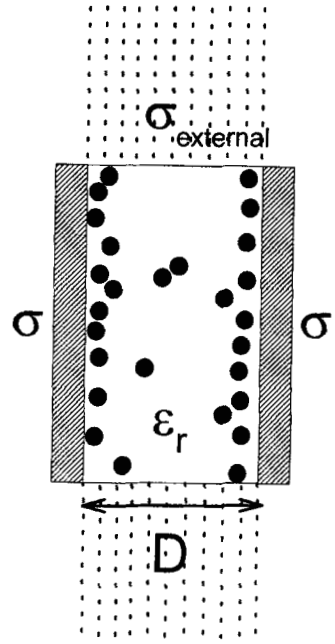

FIGURE 1 Schematic picture of the model system with uniformly charged walls enclosing the neutralizing counter-ions (see text).

virtual sheets is given by:

$$U^{is} = -\frac{q\sigma_{\text{ext}}W}{4\pi\varepsilon_0\varepsilon_r}(G(Z) + 2\pi Z) \tag{5}$$

The interaction of the walls with a virtual sheet is:

$$U^{ws} = -\frac{\sigma_w\sigma_{\text{ext}}W^3}{4\pi\varepsilon_0\varepsilon_r}(G(Z) + 2\pi Z) \tag{6}$$

This procedure leads to accurate results if the lateral extend of the simulation cell exceeds the correlation length characterizing the counterion distribution in the two directions parallel to the slabs. In order to have the total energy of the system, two other terms need to be considered. The first is the self energy of the ions which can be written as:

$$U^{\text{self-ion}} = N \cdot \frac{q^2}{8\pi\varepsilon_0\varepsilon_r R_{\text{hyd}}} \tag{7}$$

The second is the self energy of the two walls given by:

$$U^{\text{self-wall}} = \frac{\sigma_w^2 W^3}{4\pi\varepsilon_0\varepsilon_r}\left(G\left(\frac{L}{W}\right) + G(0)\right). \tag{8}$$

The two last terms are constant for a given number of ions and a given separation between the walls. They are not required in the Monte-Carlo procedure itself but are important in the study of the overall system energetics. By contrast to simulations of coulombic fluids in euclidian geometry (which necessitate long-range corrections as described above), calculations at the surface of a hypersphere [13] in four dimension are much easier to perform since a simple and exact analytical expression of the Coulomb potential is available. Moreover, in such a geometry, there is no need of periodic boundary conditions since one deals with a closed space. When using the hyperspherical approach, one must take care of the curvature effect of the space. This can be corrected by running several calculations for increasing hypersphere radius *i.e.*, for increasing number of particles. This is quite easily achieved since hypersphere calculations are not demanding in CPU effort: the plot of an averaged quantity *versus* the reciprocal of the hypersphere radius allows an accurate estimate of this quantity at the thermodynamic limit. We have used the hyperspherical method to check the validity of the euclidian approach above described. Figure 2 presents two infinite slabs map out on the hypersphere: for commodity, when the 4D-hypersphere is reduced to a 3D usual sphere, the slabs can be seen as two segments of sphere placed at the north and south poles; the counterions are free to move between the caps at the surface of the sphere. All needed

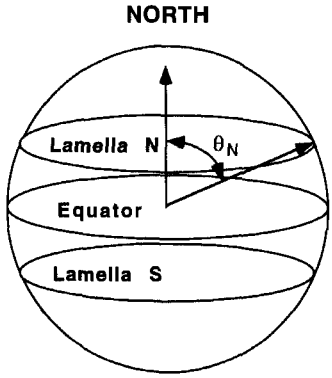

FIGURE 2 Illustration of two charged interfaces within hyperspherical geometry.

details for simulating infinite slabs in hyperspherical geometry can be found in Ref. [13].

2.1.2. *Calculation of the Force Between Two Infinite Slabs*

The force between the walls is directly related to the z-component of the pressure in the system. In Canonical Monte-Carlo simulations, this force per unit area is the osmotic pressure. The pressure between two infinite charged slabs can be derived analytically:

$$P = -\frac{\sigma_w^2}{2\varepsilon_0\varepsilon_r} + \rho_{\text{wall}}\, kT \tag{9}$$

where ρ_{wall} is the counterion density on the slabs, $\rho_{\text{wall}}\, kT$ the contact term and $[-\sigma_w^2/2\varepsilon_r\varepsilon_0]$ the electrostatic term. The pressure is however difficult to estimate accurately by using this two component expression since both contributions are of the same magnitude but of opposite sign. An alternative procedure was suggested by Gulbrand *et al.*, 15 years ago [4, 6]: these authors suggest to evaluate the pressure as the force transmitted through a fictitious plane placed at mid-distance between the slabs in the interlamellar void space; the mechanical pressure being the same everywhere in the system. With such a procedure, the z-component of the pressure can be written as the sum of three terms:

$$P = P_{\text{elec}} + P_{\text{ideal}} + P_{\text{contact}} \tag{10}$$

where P_{elec} is the electrostatic force per unit area acting across a fictitious plane at $z = 0$ (see Fig. 1), $P_{\text{ideal}} = \rho(0)kT$ is the kinetic contribution with $\rho(0)$ being the ionic density at $z = 0$ and P_{contact} is proportional to the number of ions in contact (collisions) through the plane located at $z = 0$. It has been shown that the pressure can be obtained most accurately by calculating each of its components at the midplane of the system (10). The electrostatic pressure can be obtained from the derivative with respect to the z variable of the interaction energy previously defined as the sum of the ion–ion, ion-wall and the wall–wall interactions including all long-range corrections. The contact pressure at the midplane is extrapolated from the ensemble average of $\cos(z_{ij}/r_{ij})$ of each (ij) pair of ions pertaining to different sides of the simulation box (with respect to the midplane). Finally, P_{ideal} is obtained from the ionic density in a volume $W^2\delta z$ spanning the midplane. Most of the simulations were run with 400 ions. Simulation with 1600 ions give essentially identical results as far as the total energy per ion, the pressure and the ionic profile are concerned. Figure 3 shows an excellent

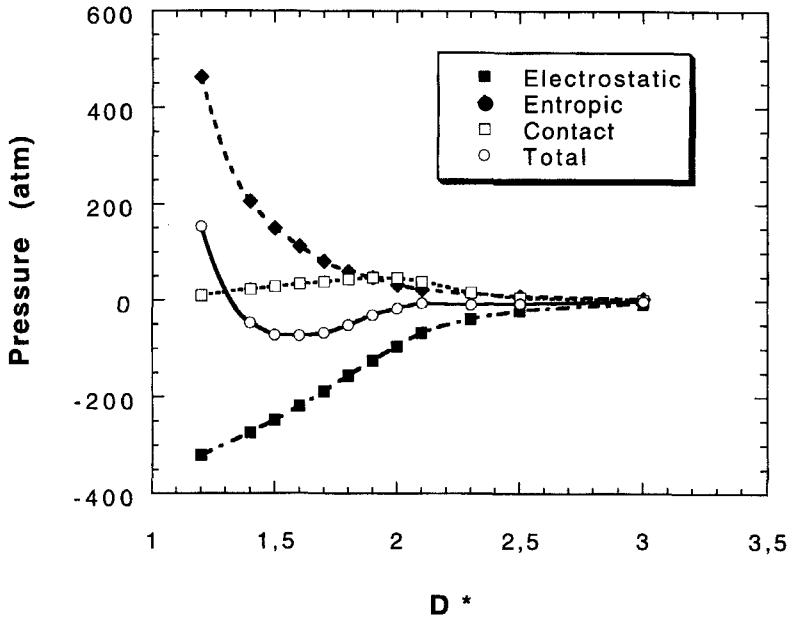

FIGURE 3 Total swelling pressure and its different components calculated for two infinite slabs (see text and [10]).

agreement between our result and those reported by Valleau *et al.* [10] for $q = +2e$, $R_{hyd} = 3\,Å$, $\varepsilon_r = 78.5$ and $\sigma_w = -1.4\ 10^{-2} e/Å^2$. It is interesting to note that (i) the electrostatic contribution to the total pressure is always negative (ii) both the ideal gas and the contact terms are positive (iii) all these three terms are strongly distance dependent. The total pressure is therefore the result of a fine balance between these three contributions.

2.2. Discoid Colloids

We have performed (N, V, T) Monte-Carlo simulations of the distribution of 842 monovalent (Fig. 4) and 421 divalent counterions neutralizing two parallel negatively charged discs [17]. The ion/ion, disc/ion and disc/disc interactions are described in the framework of the primitive model: electrostatic long-ranged coupling and hard core contact repulsion. Ion diameter is set to 4.5 Å for both counterions, corresponding to the size of hydrated sodium and calcium cations. The diameter and thickness of charged discs were set to 200 Å and 5.5 Å respectively, in order to model the behaviour of synthetic Laponite clay [20]. Each particle bears 421 negative charges

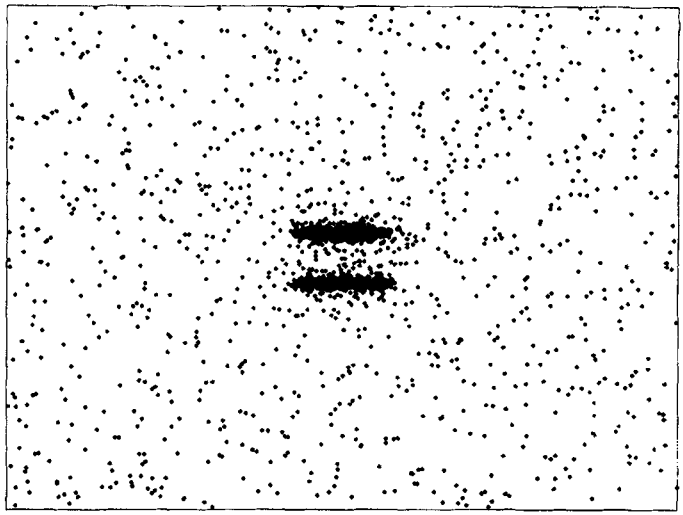

FIGURE 4 Snapshot of an equilibrium configuration of 842 monovalent counterions distributed around two charged discs.

displayed on a squared lattice within its equatorial plane. The corresponding surface charge density is 0.0067 electron per squared Å of total basal surface. In addition to the electrostatic energy, we also determined the average force acting on each particle in the longitudinal direction. This force divided by the cross section of the particle may be directly compared to the pressure determined for infinite particles. It originates from the ion/particle and particle/particle electrostatic and contact forces. The electrostatic energy is calculated by using Ewald summation [18], within the classical 3D minimum image convention. Summations in the reciprocal space are performed with 728 replica of the central cell, and the screening parameter k is set to $.005\,\text{Å}^{-1}$. Since the size of the simulation cell is 1000 Å, these conditions lead to an accuracy better than .005 for the electrostatic energy. Longitudinal contact forces exerted on each particle is determined by extrapolating to contact the local ionic densities on both sides of the disc. In order to reduce the statistical noise, 5000 blocs of 20000 iterations where necessary to thermalize and average the interparticle force.

2.3. Spherical Colloids

In this work, we present preliminary results concerning the forces between two spherical colloids neutralized by monovalent counterions (Fig. 5).

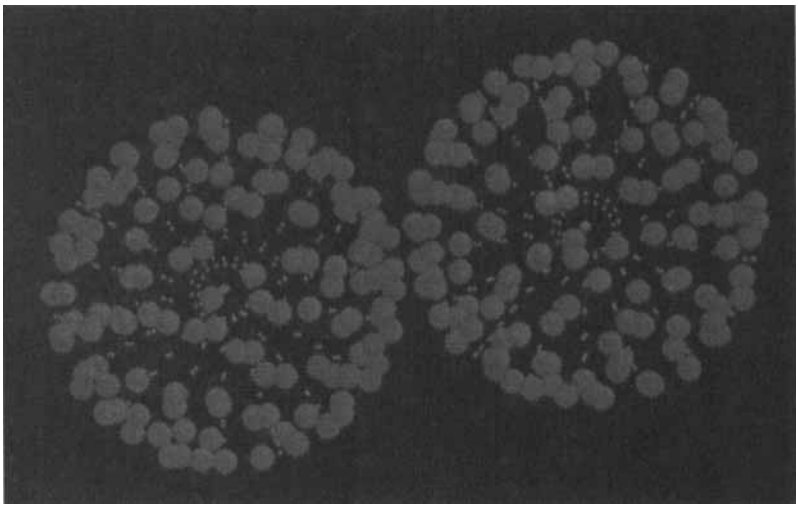

FIGURE 5 Snapshot of an equilibrium configuration of monovalent counterions distributed around two spherical colloids.

The charge of the spherical colloids is placed at their center of mass. The conditions of these simulations are those given in Table I in Ref. [16] ($\sigma = 7.3\ 10^{-5}$ e/Å^2, $q = 1$, $\varepsilon_r = 78.5$, $R_{\text{sphere}} = 554$ Å). The total force on one colloid due to the other colloid and the atmosphere of counterions is the sum of three contributions: the (repulsive) electrostatic colloid/colloid, the colloid/ion electrostatic and the contact colloid/ion terms. Both the electrostatic and contact colloid/ion terms can be calculated discretely from the standard expression in the Primitive Model and also by integrating the ionic density distribution. Both approaches give similar results (difference less than 10^{-4}) and thus provide an internal checking procedure of the code. We are seeking for the force between two isolated spherical charged colloids.

TABLE Ia Total pressure (atm) and its contact contribution for particles neutralized by monovalent counterions

	Pt	*Pcont*	*Pt*	*Pcont*
D^*	*Finite discs*		*Infinite lamellae*	
2.11	60 ± 7	61	81 ± 8	159
3.22	30 ± 7	38	32 ± 5	110
4.33	25 ± 6	25	17 ± 4	95
5.44	20 ± 6	19	11 ± 3	89
7.66	18 ± 6	14	6 ± 2	84
9.88	13 ± 6	11	3 ± 1	81
14.53	11 ± 6	9	1.7 ± .5	79.7
21.	6 ± 6	6	2.6 ± .5	80.6

Table Ib Total pressure (atm) and its contact contribution for particles neutralized by divalent counterions

D^*	*Pt*	*Pcont*	*Pt*	*Pcont*
	Finite discs		*Infinite lamellae*	
1.67	21 ± 5	66	22 ± 2	100
1.89	−7 ± 4	43	5 ± 1	83
2.11	−11 ± 3	30	−2 ± 1	76
2.33	−13 ± 3	22	−6 ± 1	72
2.56	−3 ± 6	15	−6 ± 1	72
2.78	−2 ± 10	16	−6 ± 1	72
3.00	−1 ± 7	15	−4.5 ± .5	74
3.22	2 ± 7	10	−3.2 ± .3	74.8
3.44	−1 ± 7	12	−2.5 ± .3	75.5
3.67			−0.6 ± .1	77.4
3.89			−0.6 ± .1	77.4
4.11			−0.5 ± .1	77.5
4.33			−0.3 ± .1	77.7

Therefore, we have used large simulation cell: an important aspect of this work was to check the influence of the simulation cell size on the results (periodic boundary conditions and minimum image convention were applied). We have found that equilibrium is reached if the maximum step length for random displacement is a proportion (typically 15%) of the smallest ion/colloid distance (the maximum step length varies during the course of the simulation). This allows to properly sample the very large configurational space available for reasonable simulation cell size (2000 Å); simulations run with larger simulation cell lead to same energy and pressure therefore avoiding the use of Ewald summations. By contrast, simulations based on fixed maximum step length for random translation displacement do not converge in such large simulation cells.

3. RESULTS AND DISCUSSION

3.1. Infinite Slabs

Here after, we report some pressure calculations for different value of the surface charge density (characterizing a given material) as a function of the inter-layer distance. Since the simulations were run at constant volume, a positive pressure would correspond to a swelling system *i.e.*, in a real experiment, the inter-layer distance would increase until the mechanical equilibrium is recovered. Conversely, a negative pressure indicates a cohesive system *i.e.*, in a real experiment, the inter-layer separation would decrease to compensate for this negative pressure. Figure 6 shows the variation

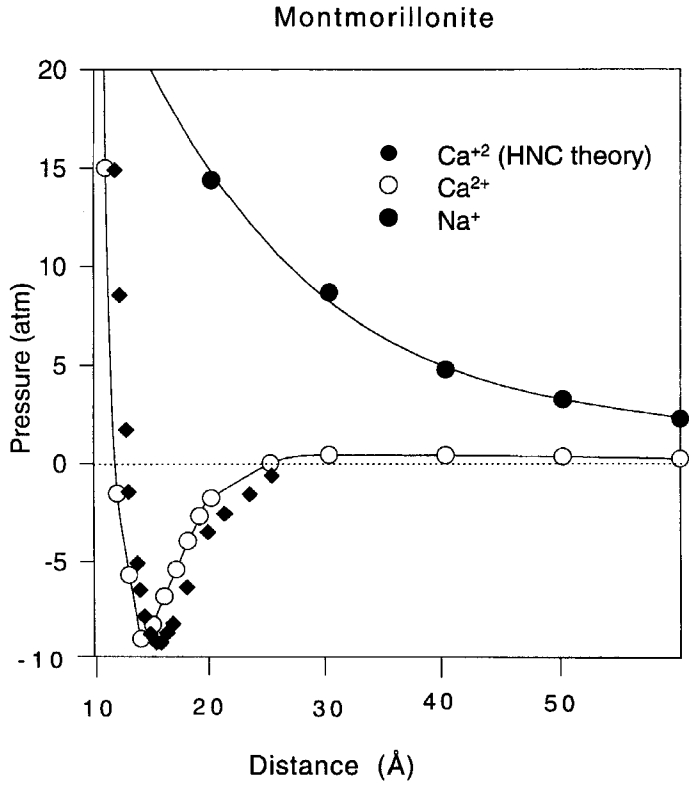

FIGURE 6 Variations of the osmotic pressure for sodium and calcium Montmorillonite.

of the osmotic pressure with the wall separation for the Ca^{2+} and Na^{+}/Montmorillonite systems respectively. It is clear that the Ca^{2+}/Montmorillonite system exhibits a cohesive behavior for distances larger than 8.5 Å. This attraction is at relatively long range (at 22 Å, the pressure is still negative) and the minimum (− 8.9 atm) is reached at 13 Å. The pressure becomes positive at 22 Å and goes through a maximum at around 27 Å before a continuous decrease. The overall behavior is in agreement with experiment although pressure oscillations at short range (solvation forces), experimentally observed [19], are not reproduced in the simulation because of the continuum approach used to describe the solvent [11]. It is also interesting to note the good agreement between the simulation results and the predictions of HNC theory [7, 8]. In the case of sodium ions in Montmorillonite, the pressure remains always positive indicating a swelling behavior [1, 2]. Figure 7 shows pressure/separation curves for the Ca^{2+} and

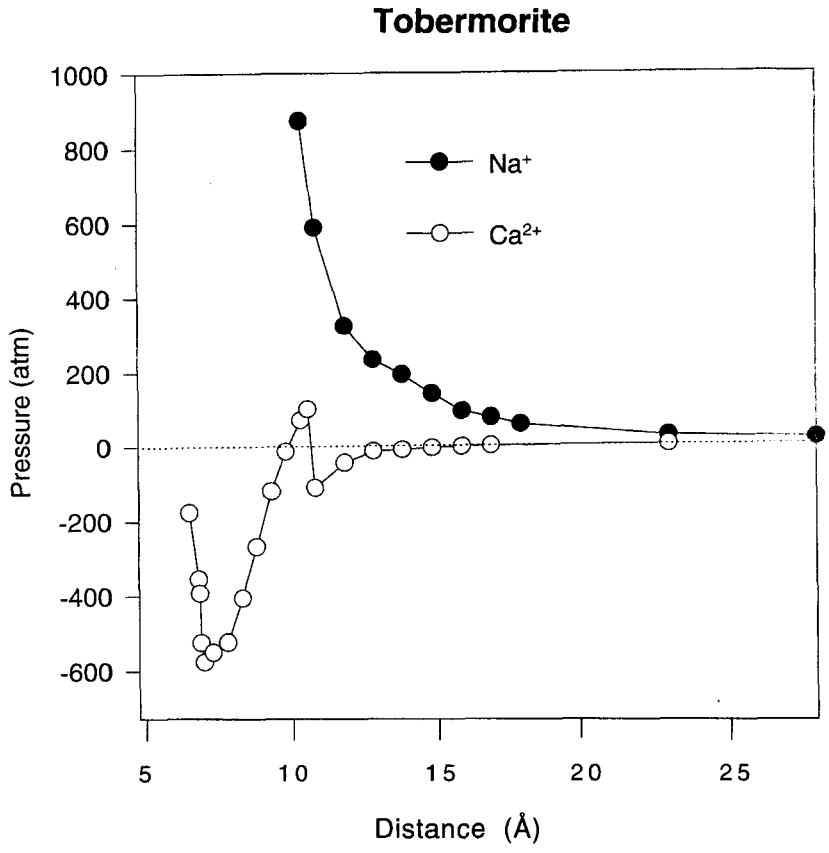

FIGURE 7 Variations of the osmotic pressure for sodium and calcium Tobermorite.

Na^+ in Tobermorite. Again the Na^+/Tobermorite system is continuously swelling while the Ca^{2+}/Tobermorite system exhibits a strong cohesive behavior with a deep minimum (−580 atm) at 7 Å. Thus this model, although simplistic is able to reproduce the observed cohesive behavior of cement materials and the swelling behavior of sodium/clays systems. Figure 8 presents a two dimensional plot of the pressure as a function of the surface charge density and of the plate separation for calcium ions. It is interesting to note the existence of a pressure minimum for an optimal value of the surface charge density $\sigma_w^{opt} = -3\,10^{-2}\,e/Å^2$ at a distance of 7 Å. The analysis of the different contributions to the pressure indicates that (i) the electrostatic pressure (negative) becomes more attractive with increasing value of σ (ii) the ideal gas term (positive) gives the largest contribution to

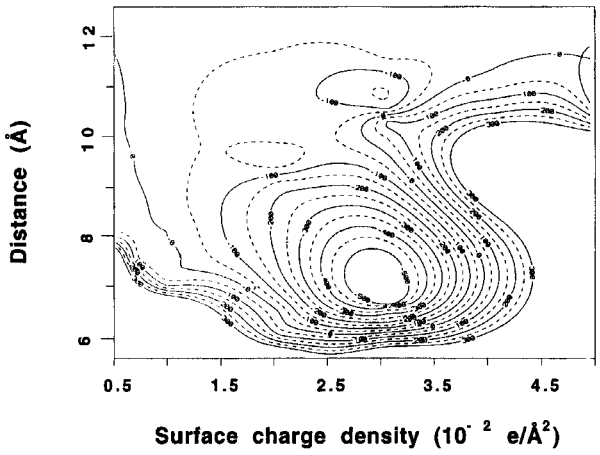

FIGURE 8 Contour map of the total pressure between two infinite charged interfaces dispersed in water and neutralized by calcium counterions.

the repulsive part of the total pressure for $\sigma < \sigma_w^{opt}$; the contact pressure being negligible (iii) conversely for $\sigma > \sigma_w^{opt}$, the contact pressure starts to increase dramatically and diverges; it becomes at $\sigma_w = -4\,10^{-2}\,e/Å^2$, the main component of the repulsive part of the total pressure. The deep pressure minimum obtained at $\sigma_w = \sigma_w^{opt}$, progressively vanishes and the pressure becomes positive for $\sigma_w = -3.9\,10^{-2}\,e/Å^2$ for an inter-layer separation of 7 Å. We also note the existence of a secondary minimum for values of σ_w close to σ_w^{opt} (see also Figs. 9 and 10). This is the consequence of the brutal vanishing of the contact pressure when the layer separation allows the formation of two distinguishable counter-ion layers. The absolute distance between the layers is then equal to two ionic diameters. The existence of a deep minimum at short distance thus corresponds to a situation in which it is not possible to define two distinct electric double layers. A more detailed picture of the interaction between charged layers should include both the atomic roughness of the surfaces and a molecular description of the solvent in order to describe phenomena such as solvation forces [11]. As shown in Eq. (9), the total pressure can be written as a sum of an electrostatic contribution with a contact term which depends on the ionic density at contact on the slabs. This equation always leads to a repulsive behavior in the framework of the Poisson-Boltzmann theory (PB) which neglects ionic correlations. In the PB context, Eq. (9) simply reduces to the entropic component of Eq. (10) ($\rho(0)\,kT$). The difference in the ionic profile between the results as obtained within the PB framework and the MC

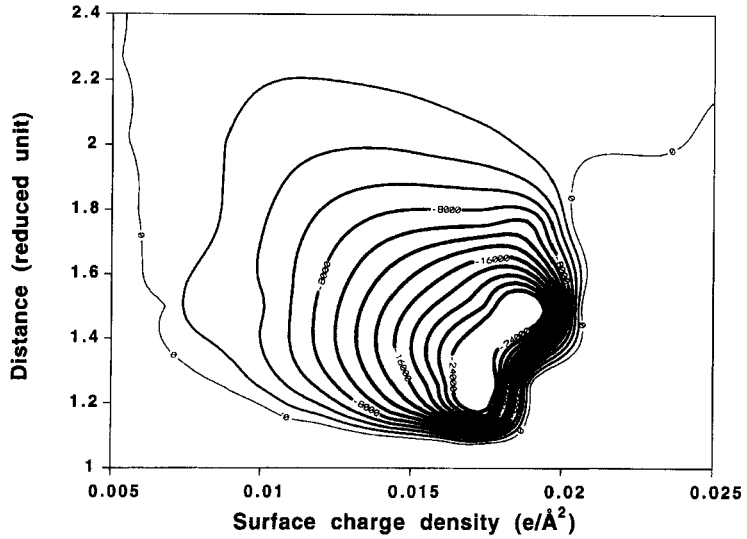

FIGURE 9 Contour map of the total pressure between two infinite charged interfaces dispersed in water and neutralized by divalent counterions with a diameter of 2 Å.

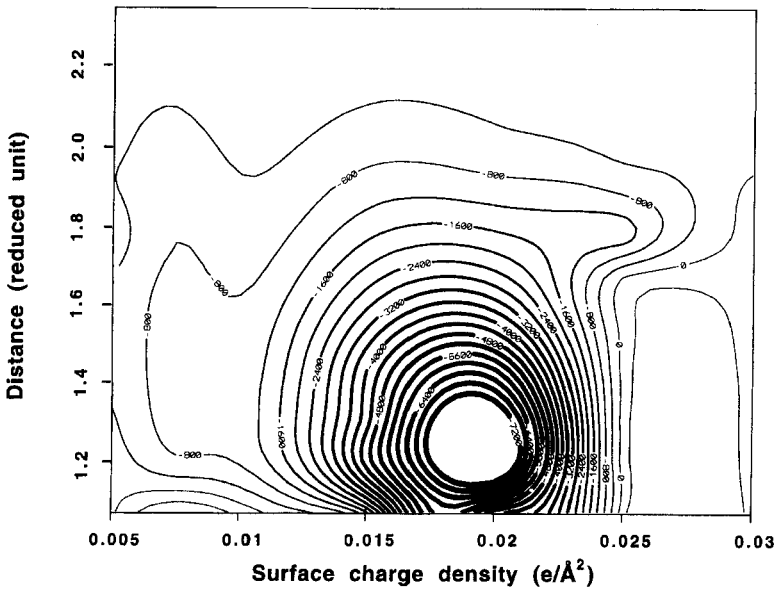

FIGURE 10 Contour map of the total pressure between two infinite charged interfaces dispersed in organic solvent ($\varepsilon_r = 5$) and neutralized by monovalent counterions with a diameter of 4.25 Å.

simulations (which into account *de facto* ionic correlation effects) are shown in Figure 11. At weak coupling (Na^+/montmorillonite), the PB concentration profile coincides with that obtained from the MC simulation. Note also, the small amplitude of the fluctuations in the instantaneous profile calculated from a single equilibrium configuration: this criterium (small fluctuations) matches the condition of validity of a mean field approximation such as the PB theory. A larger electrostatic coupling (Ca^{2+}/Tobermorite), larger fluctuations occur and the PB profile is very different from that obtained with the simulations. To further illustrate the ionic correlation effect, we have also calculated 2D-radial distribution functions of monovalent counterions confined between charged lamellae ($\sigma_w = 5.5\ 10^{-2}$ e/Å^2) and reduced separation $L^* = L/d = 1.78$ (Fig. 12). The 2D internal radial distribution function is calculated within the plane of counter-ions

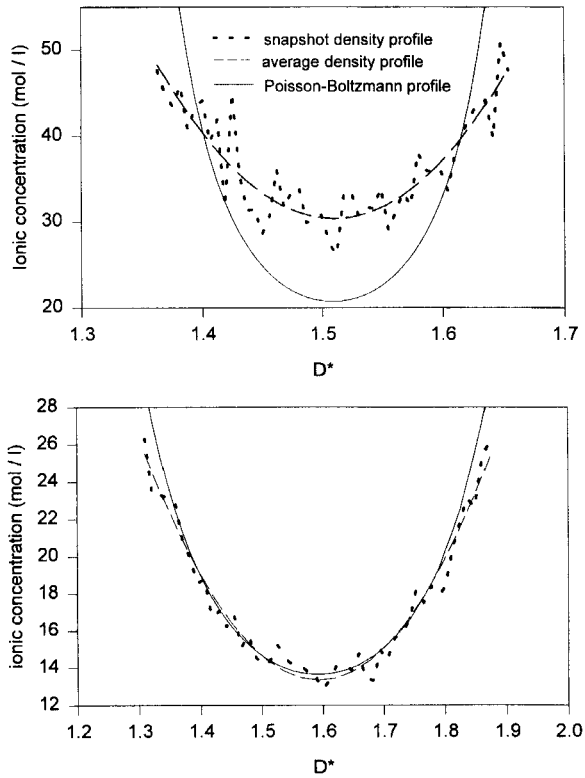

FIGURE 11 Comparison between the Poisson-Boltzmann concentration profiles of confined counterions and the instantaneous and averaged Monte-Carlo results calculated for the Ca/Tobermorite (a) and Na/Montmorillonite (b) interfaces.

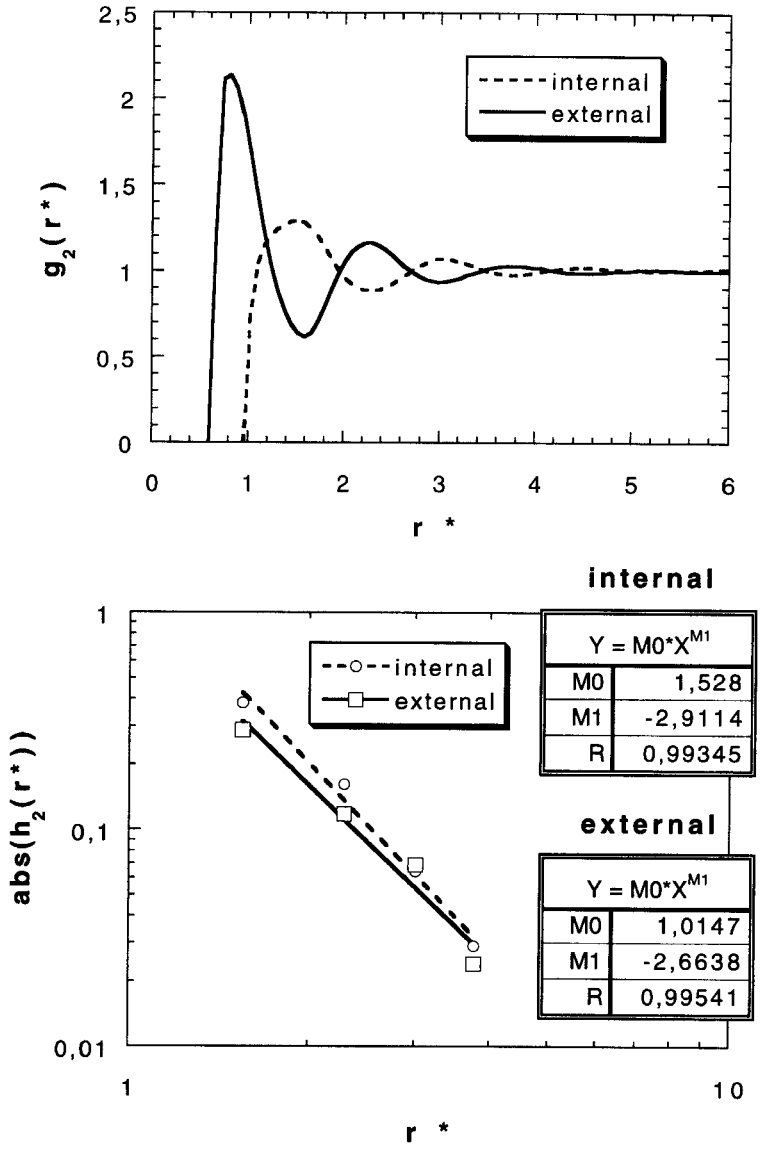

FIGURE 12 2D radial distributions functions of confined counterions (a) (see text) and its extrema (b).

condensed at contact with one single charged slab while the external one is evaluated between two facing layers of condensed counter-ions. Clearly, Figure 12 exhibits strong correlations in both internal and external radial

distribution functions due to excluded volume effect. This local ordering propagates at large distance following an algebraic decay law as predicted by Jancovici [12] for 2D systems.

At plate separations lower than two ionic diameters, Figures 8–10 exhibit two transitions from repulsive to attractive mechanical behavior of infinite charged interfaces. Despite of the complexity reported on these contour maps, one may be tempted to renormalize these results by introducing a master equation of state. By contrast with continuous potentials frequently used in numerical simulations (Lennard-Jones, Morse, Yukawa, Buckingham,...) the primitive model, at the basis of these results, mixes discontinuous hard-core repulsion with continuous long range electrostatic attracto-repulsive potentials. Because of the singularity of the hard-core potential, the research of a master curve renormalizing Figures 8–10 (and also 2D pressure contour maps in reference [14]) appears as a hopeless quest. Nevertheless we have tried to deduce some necessary conditions for the existence of interlamellar attraction.

As seen in Eq. (10), the mechanical behavior of infinite charged lamellae is better described as a balance between entropic repulsion, electrostatic attraction and ion–ion contact repulsion (evaluated at midplane). At low surface charge density, electrostatic and contact interionic correlations are negligible and the mechanical behavior of the interface is driven by entropic repulsion. This regime corresponds to the domain of validity of the Poisson-Boltzmann treatment, which neglects ionic correlations (see Fig. 11). At higher surface charge density, electrostatic correlations emerge leading to a net attraction. Finally, at very large surface charge density, the mechanical behavior of the charged interface is overcome by the repulsive hard-core contributions. In order to predict these successive transitions between attracto/repulsive regimes, let us introduce two parameters:

$$\xi = \frac{|\sigma_w q| R_{\text{hyd}}}{4\pi\varepsilon_0\varepsilon_r kT} \tag{11}$$

ξ is proportional to the coupling parameter quantifying the strength of the counterion/lamella electrostatic attraction at contact;

$$\eta = \frac{8\pi|\sigma_w| R_{\text{hyd}}^3}{3L|q|} \tag{12}$$

η is the volume fraction of the counterions confined between the lamellae which quantifies the strength of the ion–ion contact repulsion.

From the analysis of Figures 8–10 one concludes that the pressure minimum occurs for reduced interlamellar separation $L^* = L/(2R_{hyd}) \sim 1.45$. We thus analyse the transitions between attracto/repulsive regimes at this optimum separation, since the absence of attraction at this critical separation is a condition sufficient to preclude the occurence of a net attraction between the lamellae, whatever their separation. From the analysis of Figures 8–10, we note that the first transition between entropic repulsion and electrostatic attraction is monitored by the electrostatic coupling parameter and occurs at $L^* = 1.45$ for $\xi = (0.4 \pm 0.15)$. The second transition between electrostatic attraction and contact repulsion is monitored by the volume fraction of counterions and occurs at $L^* = 1.45$ for $\eta = (0.29 \pm 0.03)$. From the definition of these two parameters (Eqs. 11 and 12), one deduces the conditions necessary for the existence of an attractive regime at $L^* = 1.45$:

$$(0.45 \pm 0.15)\frac{4\pi\varepsilon_0\varepsilon_r kT}{|q|R_{hyd}} \leq |\sigma_w| \leq (0.10 \pm 0.01)\frac{|q|}{R_{hyd}^2} \tag{13}$$

Furthermore we note that the pressure minimum occurs for a counterion volume fraction $\eta^{opt} = (0.251 \pm 0.002)$, leading to the optimum surface charge density $|\sigma^{opt}| = (0.087 \pm 0.001)\,|q|/R_{hyd}^2$. By using Eq. (9), it is possible to deduce from the average ionic density at $L^* = 1.45$ the local counterion density at contact with the charged lamellae: $\rho_{wall} = (7 \pm 3)\,\rho^\circ$ (ρ° is the average density of confined counter-ions). As a consequence, the pressure minimum may be estimated by:

$$P^{opt} = -\frac{(\sigma^{opt})^2}{2\varepsilon_0\varepsilon_r} + (7 \pm 3)\rho^\circ kT \tag{14}$$

As shown on Figure 13, we obtain a semi-quantitative agreement between the predicted and calculated optimal charge densities and pressures. As a conclusion, we are only able to deduces the necessary conditions for the existence of an attractive regime. We further predict the strength of the optimum attraction between the charged lamellae and its corresponding surface charge density. Such information may be very useful in material science for optimizing the mechanical properties of charged interfaces. Obviously, the validity of our predictions are restricted by the limitations of the primitive model and the limited number of parameters investigated in this study (counterion charge equal to 1 or 2, dielectric constant equal to 5 or 78.5 and surface charge densities varying between $5\,10^{-4}$ and $6\,10^{-2}$ e/Å^2). While these parameters cover a wide range encountered by most real

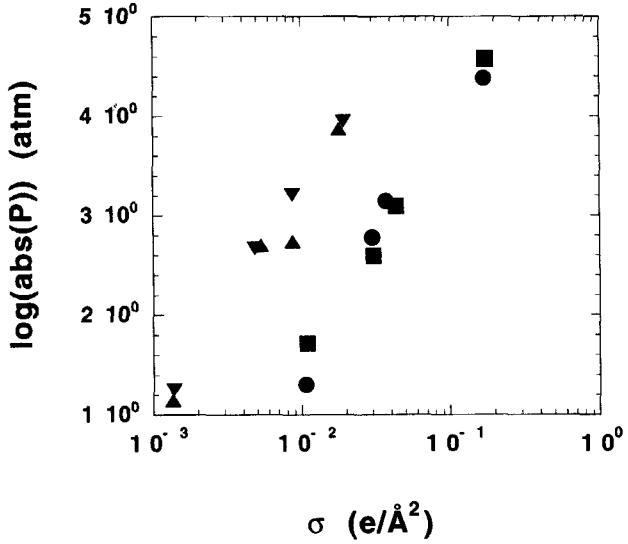

FIGURE 13 Comparison between the optimal pressure obtained from numerical simulations (• and ▲) and its derivation from Eq. (14) (■ and ▼) (see text) calculated for divalent counterions in water (ε_r = 78.5; ■ and •) and for monovalent counterions in organic solvent (ε_r = 5, ▲ and ▼).

materials, it should be interesting to investigate other systems, including, as an example, counterions with larger valency.

3.2. Discoid Colloids

Average concentration profiles are drawn on Figure 14 for ions located in a cylinder limited by the cross section of the discs. Since the origin is set at the center of each disc, the densities of counterions at contact with the disc basal surfaces is obtained by extrapolating the concentration profiles down to a distance of 5 Å. Figure 14 exhibits noticeable differences between the local ionic concentrations inside and outside the interparticle domains. The ionic densities are always larger in the interparticle domain because of the overlap of the electrostatic well located in the vicinity of each particle, leading to ionic condensation. One can divide the simulation cell in two domains: the inner and outer disc domains. By contrast to infinite slabs, the difference between the ionic distributions in these domains triggers the overall mechanical behavior of the system: the net contact force acting on each particle results from a balance between its inner and outer ionic contact densities. We have calculated the net force exerted on each particle from

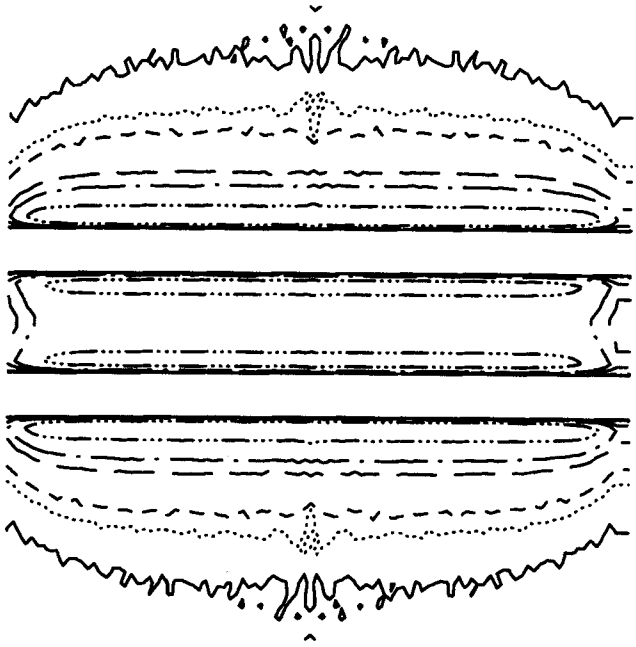

FIGURE 14 Average local concentration of monovalent counterions distributed around two charged discs $(c_i(\mathbf{r})/c_i^\circ = 3000[- \cdots -], 1000\,[— \cdot —], 500\,[— —], 100\,[- - -], 50\,[\ldots], 10[—])$.

thermalized ionic distributions. The results are shown on Figure 15 for discs neutralized by mono- and di-valent counterions. The net force is divided by the cross section of the disc in order to be compared with the pressure calculated previously for infinite charged lamellae [13, 14]. Because of the finite size of the particles, counterions are located on both sides. It follows that the net contribution of the ion/disc longitudinal electrostatic and contact forces cannot be predicted *a priori*. However, because of the dissymmetry reported in Figure 14, one may conclude to a net repulsive ion/disc contact force.

The results shown on Figure 15 are in qualitative agreement with the data previously reported for infinite charged lamellae [13, 14]. For infinite lamellae neutralized by mono- and di-valent counterions, the net longitudinal pressure resulted from the balance between large electrostatic attraction and contact repulsion (see Eq. (9)). For finite particles neutralized by monovalent counterions, the electrostatic contribution is always negligible (see Tab. I), and the net longitudinal force results mainly from the repulsive contact force, because of the excess of condensed counterions in

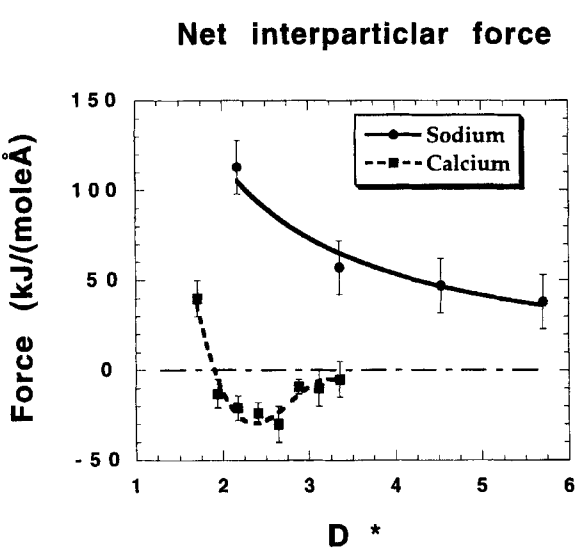

FIGURE 15 Total pressure (see text) exerted between two charged discs neutralized by monovalent and divalent counterions.

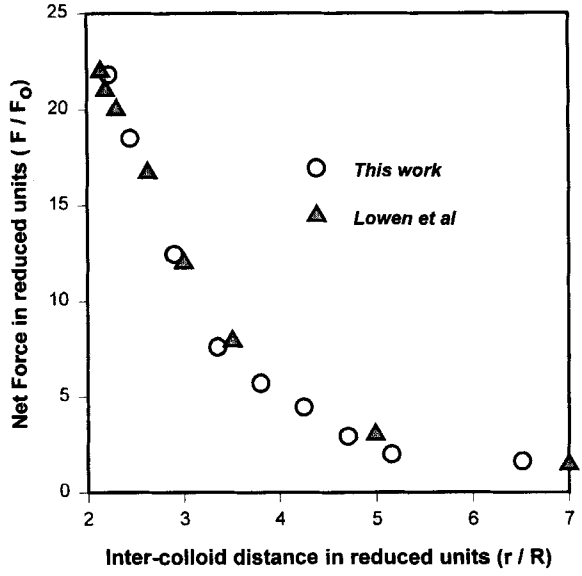

FIGURE 16 Total force exerted between two spherical colloids neutralized by monovalent counterions (Löwen *et al.* [16]).

the inner domain. For charged discs neutralized by divalent counterions, the contact contribution to the longitudinal force is still repulsive, but the electrostatic attraction becomes significant and may overcome the contact repulsion, leading to attracto/repulsive behavior. This attraction is responsible for the flocculation reported for dilute suspensions of such colloidal anisotropic particles in presence of divalent counterion [8]. Finally, at large separation the contact force between two finite discs becomes negligible, since the local ionic concentration are the same at both sides of the discs. Note that totally different behavior is reported for infinite charged lamellae.

3.3. Spherical Colloids

Figure 16 presents the force *versus* distance for two spherical colloids neutralized by monovalent counter-ions (sodium). Clearly, in the conditions as above described, the two colloids repel each other. Our results are in excellent agreement with those reported by Allahayrov *et al.* [16]. This repulsion is due by the ion/colloid electrostatic term (the colloid/colloid term being obviously also repulsive). Note that the colloid/ion contact term is found negligible.

4. CONCLUSIONS

We have studied the long range electrostatic interaction between charged colloids of various geometries (infinite slabs, discoids and spheres) in various coupling conditions. We have demonstrated the existence of large attractive domains for infinite slabs at sufficient electrostatic coupling conditions at variance with Poisson-Boltzmann predictions. This attraction results from ionic correlation forces. Note that the attractive behavior disappears at very high coupling due to contact forces. By introducing two coupling parameters which quantify both the electrostatic and contact forces, we were able to formulate necessary conditions for the existence of an attractive regime. We have further investigated the influence of the finite size effect of colloids on their mutual interactions. We have found an attractive behavior between two discoid colloids at large coupling conditions driven by electrostatics. At low coupling, repulsion is detected and driven by contact forces. Preliminary calculations on spheres indicate a repulsive behavior at low coupling conditions.

Acknowledgments

It is a pleasure to cordially thank Drs. H. van Damme, J. M. Caillol and J.-L. Raimbault for their collaboration and interest to the progress of this work. Numerical simulations were performed either on Cray supercomputer (IDRIS, Orsay, France) or locally on workstations purchased thanks to grants from Région Centre (France).

References

[1] Buscall, R., Goodwin, J. W., Hawkins, M. W. and Ottewill, R. H. (1982). "Visco-elastic properties of concentrated lattices", *J. Chem. Soc. Faraday Trans.*, **1**, 2889–2899.
[2] Bradbury, A., Goodwin, J. W. and Hughes, R. W. (1985). "Deformation melting and relaxation of structured colloidal dispersions", *Langmuir*, **8**, 2863–2872.
[3] Palberg, T., Hartl, W., Wittig, U., Versmold, H. and Wurth E. Simmacher (1992). "Continuous deionization of latex suspensions", *J. Phys. Chem.*, **96**, 8180–8183.
[4] van Megen, W. and Snook, I. (1980). "The Grand-Canonical Ensemble Monte-Carlo method applied to the electrical double layer", *J. Chem. Phys.*, **73**, 4656–4662.
[5] Linse, P. and Jönsson, B. (1983). "A Monte-Carlo study of the electrostatic interaction between highly charged aggregates. A test of the cell model applied to micellar systems", *J. Chem. Phys.*, **78**, 3167–3176.
[6] Gulbrand, L., Jönsson, B., Wennerström, H. and Linse, P. (1984). "Electrical double layer forces. A Monte-Carlo study", *J. Chem. Phys.*, **80**, 2221–2228.
[7] Kjellander, R., Marcelja, S. and Quirk, J. P. (1988). "Attractive double-layer interaction between calcium clay particles", *J. Coll. Int. Sci.*, **126**, 194–211.
[8] Kjellander, R., Marcelja, S., Pashley, R. M. and Quirk, J. P. (1988). "A theoretical and experimental study of forces between charged mica surfaces in aqueous $CaCl_2$ solutions", *J. Phys. Chem.*, **92**, 6489–6492.
[9] Delville, A. and Laszlo, P. (1989). "Simple results on cohesive energies of clays from a Monte-Carlo calculation", *New J. Chem.*, **13**, 481–491.
[10] Valleau, J. P., Ivkov, R. and Torrie, G. M. (1991). "Colloid stability: the forces between charged surfaces in an electrolyte", *J. Chem. Phys.*, **95**, 520–532.
[11] Delville, A. (1993). "Structural properties of confined liquids: A molecular model of the clay-water interface", *J. Phys. Chem.*, **97**, 9703–9712.
[12] Jancovici, B. (1992). "Inhomogeneous 2D plasma", In: *Fundamentals of Inhomogeneous Fluids*, Henderson, D. and Dekker, M., Eds., New York, p. 201.
[13] Delville, A., Pellenq, R. J.-M. and Caillol, J.-M. (1997). "A Monte-Carlo (N, V, T) study of the stability of charged interfaces: a simulation study on a hypersphere", *J. Chem. Phys.*, **106**, 7275–7285.
[14] Pellenq, R. J.-M., Caillol, J.-M. and Delville, A. (1997). "Electrostatic attraction between two charged surfaces: A (N, V, T) Monte-Carlo simulation", *J. Phys. Chem. B*, **101**, 8584–8594.
[15] Delville, A., Gasmi, N., Pellenq, R. J.-M., Caillol, J.-M. and Van Damme, H. (1998). "Correlations between the stability of charged interfaces and ionic exchange capacity: a Monte-Carlo study", *Langmuir*, **14**, 5077–5082.
[16] Allahyarov, E., D'Amico, I. and Löwen, H. (1998). "Attraction between like-charged macroions by coulomb depletion", *Phys. Rev. Lett.*, **81**, 1334–1337.
[17] Delville, A. (1999). "(N, V, T) Monte-Carlo simulation of the electrostatic interactions between charged colloids: finite size effects", *J. Phys. Chem.*, **B103**, 8296–8300.
[18] Heyes, D. M. (1994). "Pressure tensor of partial charge and point dipole lattices with bulk and surface geometries", *Phys. Rev. B*, **49**, 755–764.
[19] Israelachvili, J. N. (1985). *Intermolecular and Surface Forces*, Acad. Press, New York.
[20] Maurchid, A., Delville, A., Lambard, J., Lecolier, E. and Levitz, P. (1995). "Phase diagram of colloidal dispersions of anisotropic charged particles: equilibrium properties, structure and rheoligy of Laponite suspensions", *Langmuir*, **11**, 1942–1950.